Measurement of the N^{*-}-N^{*++} Mass Difference*

GEORGE GIDAL,† ANNE KERNAN, AND SEDONG KIM
Lawrence Radiation Laboratory, University of California, Berkeley, California
(Received 1 June 1965; revised manuscript received 8 September 1965)

A measurement of the N^{*-}-N^{*++} mass and width differences is described, where N^* is the nucleon resonance with $I(J^P)=\frac{3}{2}(\frac{3}{2}^+)$ and mass approximately 1240 MeV. The resonances were produced in the inelastic reactions $n\,n\to p\,n\,\pi^-$ and $p\,p\to n\,p\,\pi^+$, which are known to proceed almost entirely via N^{*-} and N^{*++} production, respectively, in the observed energy region. A comparison of the $(n\pi^-)$ and $(p\pi^+)$ effective-mass distributions gives a mass difference of 7.9 ± 6.8 MeV and a width difference of 25 ± 23 MeV for N^*-N^{*++}. This result agrees with predictions based on the $SU(3)$ and $SU(6)$ symmetry schemes.

We report here a measurement of the N^{*-}-N^{*++} mass difference[1] $\delta\omega_0$ and width difference $\delta\Gamma_0$. N^* is the nucleon resonance of isotopic spin $\frac{3}{2}$, $J^P=\frac{3}{2}^+$, and mass approximately 1240 MeV.

The resonances were produced in the inelastic reactions

$$nn\to p_1n_2\pi_3^-\,, \tag{1}$$

$$pp\to n_1p_2\pi_3^+\,, \tag{2}$$

at a mean c.m. energy of 2.35 BeV. At this energy reactions (1) and (2) are known to proceed almost entirely via N^{*-} and N^{*++} production, respectively.[2,3] We determined $\delta\omega_0$ and $\delta\Gamma_0$ by a comparison of the distributions in the invariant mass ω_{23} for both reactions.

In the $SU(3)$ symmetry scheme N^* is a member of the $J^P=\frac{3}{2}^+$ decouplet, along with Y^*, Ξ^*, and Ω^-. Okubo[4] has recently pointed out that, because of electromagnetic mass splitting, the Gell-Mann–Okubo[5] mass formula is valid only for particles with the same charge, and in particular a knowledge of the N^{*-} mass is required for the comparison $\Omega^--\Xi^{*-}=\Xi^{*-}-Y^{*-}=Y^{*-}-N^{*-}$. (We use the symbol for a particle as a symbol for its mass also.) The decay width of N^{*-} is also needed to test the predicted relationship between decay amplitudes of the decouplet particles Ξ^*, Y^*, and N^*.[6] In addition, the measured mass difference can be compared with the predictions of the various symmetry schemes.

In Sec. I of the paper the predictions of electromagnetic mass splittings within the framework of the $SU(3)$ and $SU(6)$ symmetry schemes are discussed. Section II contains the experimental details, and Sec. III considers possible systematic errors in the data. Section IV presents the results, and discusses the problem of elucidating resonance parameters from plots of invariant mass. In Sec. V the experimental measurement is compared with predictions based on the $SU(3)$ and $SU(6)$ symmetry schemes.

I. ELECTROMAGNETIC MASS SPLITTING

The masses of particles within a given $SU(2)$ representation are believed to be identical in the limit of isotopic spin invariance. The electromagnetic force removes this degeneracy, giving rise to mass differences of the order of αm_π (α is the fine-structure constant). In principle, the mass differences within an isomultiplet are obtainable by a calculation of the electromagnetic self-energies of the particles therein. The attempts to calculate self-energies for strongly interacting particles, within the framework of a perturbative expansion of field theory, have been unsuccessful.

In the unitary symmetry scheme isomultiplets of different hypercharge are grouped into "supermultiplets" (or unitary multiplets) which are the irreducible representations of the $SU(3)$ group. It is postulated that, in the limit of exact unitary symmetry, the masses of all particles within a given $SU(3)$ representation are identical. The observed mass differences between isomultiplets within a unitary multiplet are of the order of 100 MeV, and are believed to arise from the "medium-strong" force. By making the assumption that unitary symmetry is violated only by the electromagnetic interaction, it is possible to relate the mass splittings within different isomultiplets of a supermultiplet. In the baryon octet, for example, the prediction[7] of $\Xi^--\Xi^0=\Sigma^--\Sigma^++p-n$ has been experimentally confirmed.[8] For the $\frac{3}{2}^+$ decouplet, of which N^* is a member, the relationship

$$m=m_0+aQ+bQ^2 \tag{3}$$

* Work performed under auspices of U. S. Atomic Energy Commission.
† Presently on research leave at Istituto di Fisica dell' Universitá, Torino, Italy.
[1] A preliminary result of this experiment was presented at the 1964 International Conference on High Energy Physics, Dubna, U. S. S. R.
[2] R. Birge, R. Ely, G. Gidal, G. Kalmus, A. Kernan, and S. Kim, Lawrence Radiation Laboratory Report UCRL-11550, 1964 (unpublished).
[3] D. V. Bugg, A. J. Oxley, J. A. Zoll, J. G. Rushbrooke, V. E. Barnes, J. B. Kinson, W. P. Dodd, G. A. Doran, and L. Riddiford, Phys. Rev. **133**, B1017 (1964).
[4] S. Okubo, J. Phys. Soc. Japan **19**, 1507 (1964).
[5] M. Gell-Mann, Phys. Rev. **125**, 1067 (1962); S. Okubo, Progr. Theoret. Phys. (Kyoto) **27**, 949 (1962).
[6] C. Becchi, E. Eberle, and G. Morpurgo, Phys. Rev. **136**, B808 (1964).
[7] S. Coleman and S. L. Glashow, Phys. Rev. Letters **6**, 423 (1961).
[8] D. Carmony, G. Pjerrou, P. Schlein, W. Slater, D. Stork, and H. Ticho, Phys. Rev. Letters **12**, 482 (1964), and other recent data cited therein; L. Jauneau, D. Morellet, U. Nguyen-Khac *et al.*, Phys. Letters **4**, 49 (1963).

is predicted,[9] where Q is the charge and a and b are constants.

Coleman and Glashow have noted that the mass splittings within an $SU(3)$ supermultiplet follow an octet pattern, and have proposed a dynamical theory of unitary symmetry violation, namely that symmetry-breaking processes are dominated by "tadpole" diagrams because of the existence of an octet of scalar mesons.[10] For the $\frac{3}{2}^+$ decouplet such an octet dominance leads to an "equal-spacing" rule for electromagnetic splitting,

$$N^{*++}-N^{*+}=N^{*+}-N^{*0}=N^{*0}-N^{*-}=Y^{*+}-Y^{*0}=Y^{*0}-Y^{*-}=\Xi^{*0}-\Xi^{*-}.$$

It also gives an intramultiplet relationship

$$(N^{*++}-N^{*+})/(N^{*}-Y^{*})=(\Sigma^{+}-\Sigma^{-})/(N-\Xi),$$

which yields $N^{*++}-N^{*+}=-3.0$ MeV and $N^{*++}-N^{*-}=-9.1$ MeV. These predictions must, however, be modified by the contributions of other mass-splitting diagrams. The leading nontadpole contribution to the electromagnetic self-masses of baryons comes from intermediate states containing one baryon and one photon.[11] The tadpole and nontadpole contributions to the electromagnetic mass differences are shown in Table I.

Dashen and Frautschi have proposed a bootstrap mechanism to explain octet dominance of the mass splitting.[12] Higher order effects in this model again reduce the splitting and alter the equal-spacing pattern.

The group $SU(6)$ contains both $SU(2)$ and $SU(3)$ as subgroups. In the recently proposed $SU(6)$ symmetry scheme the baryon octet and the $J^P=\frac{3}{2}^+$ decouplet are assigned to the 56-dimensional representation of $SU(6)$.[13] The relations between the 10 mass differences in the 56-dimensional representation have been derived in the limit where $SU(6)$ symmetry is broken by electromagnetism only[14]:

$$\begin{aligned}\Xi^{-}-\Xi^{0}&=(\Sigma^{-}-\Sigma^{+})-(n-p),\\ N^{*0}-N^{*+}&=Y^{*0}-Y^{*+}=n-p,\\ &=(n-p)+(\Sigma^{-}+\Sigma^{+}-2\Sigma^{0}),\\ N^{*-}-N^{*++}&=3(n-p).\end{aligned} \quad (4)$$

The relationships between the decouplet members are identical with Eq. (3).

[9] S. P. Rosen, Phys. Rev. Letters **11**, 100 (1963); A. J. MacFarlane and E. C. G. Sudarshan, Nuovo Cimento **31**, 1176 (1964).
[10] S. Coleman and S. L. Glashow, Phys. Rev. **134**, B671 (1964).
[11] R. Socolow, Ph.D. thesis, Harvard University, 1964 (unpublished).
[12] R. Dashen and S. Frautschi, Phys. Rev. Letters **13**, 497 (1964) and Phys. Rev. **137**, B1331 (1965).
[13] F. Gürsey and L. A. Radicati, Phys. Rev. Letters **13**, 173 (1964); A. Pais, *ibid.* **13**, 175 (1964); B. Sakita, Phys. Rev. **136**, B1756 (1964).
[14] T. K. Kuo and Tsu Yao, Phys. Rev. Letters **14**, 79 (1965).

TABLE I. Tadpole and nontadpole contribution to the electromagnetic mass differences.

Mass difference	A[a]	B[b]	C[c]
$N^{*++}-N^{*+}$	−3.0	0.2	4.4
$N^{*++}-N^{*0}$	−6.1	−2.9	2.7
$N^{*++}-N^{*-}$	−9.1	−9.1	−4.9
$Y^{*+}-Y^{*0}$	−3.0	−2.8	−1.4
$Y^{*+}-Y^{*-}$	−6.1	−9.1	−9.1
$Y^{*0}-Y^{*-}$	−3.0	−6.2	−7.6
$\Xi^{*0}-\Xi^{*-}$	−3.0	−6.3	−7.7

[a] A is the tadpole term alone.
[b] B is the tadpole term plus the self-energy diagrams with a baryon octet member and a photon in the intermediate state. (See Ref. 11, p. 95.)
[c] C comprises B plus an estimate of the contribution to the self-energy diagrams from the decouplet channel. (See Ref. 11, p. 102.)

II. EXPERIMENTAL DETAILS

Two conditions are desirable to achieve a precise measurement:

(a) Reactions (1) and (2) should occur under identical experimental conditions.
(b) Both reactions should occur at the same energy.

Condition (b) is necessary because the shape of the invariant-mass plot depends on the production mechanism, and no quantitative description of the production mechanism as a function of energy is available. By observing N^* production in charge-symmetric reactions at the same energy one ensures that any difference in the invariant-mass plots is due to electromagnetic effects only.

The reactions were simultaneously achieved at the same energy and under identical experimental conditions by the interactions of a beam of 3.64-BeV/c separated deuterons[15] with deuterium in the Brookhaven National Laboratory 20-in. bubble chamber. In the majority of d-d collisions one nucleon in each deuteron is a spectator. Reactions (1) and (2) occurred in the interactions

$$dd\to p_s{}^T p_s{}^B p_1 n_2 \pi_3{}^- \quad (1a)$$

and

$$dd\to n_s{}^T n_s{}^B n_1 p_2 \pi_3{}^+, \quad (2a)$$

respectively; the subscript s denotes a spectator, either in the beam deuteron B or the target deuteron T.

A. Selection of Events

In reaction (1a) the target spectator proton is not seen in the bubble chamber in 70% of the interactions because its momentum is less than 90 MeV/c. Therefore, we scanned for events with three outgoing charged particles, since the proton in the target deuteron is then clearly a spectator. All told, 2870 events were

[15] C. Baltay, J. Sandweiss, J. Sanford, H. Brown, M. Webster, and S. Yamamoto, in *Proceedings of the 1962 Conference on Instrumentation for High Energy Physics, CERN, 1962* (North-Holland Publishing Company, Holland, 1962); J. Leitner, G. Moneti, and N. P. Samios, in *ibid.*

measured and constrained to the hypothesis:

$$dn \rightarrow pp n \pi^-, \tag{1b}$$

assuming that the target neutron was at rest in the laboratory system. In addition to reaction (1a), the (1b) events include the pn reactions: $dd \rightarrow n_s{}^B p_s{}^T pp\pi^-$. The subtraction of p_n events from the sample is described below.

Reaction (2a) was found by scanning for events with two emergent positively charged particles, of which one is a π^+ meson. In reaction (1a) the maximum π^--meson momentum is 900 MeV/c and its mean value is 350 MeV/c, and the π^+ meson in (2a) is thus readily identified by momentum and bubble density. All together, 1687 events were measured, and were constrained to reaction (2) with a beam proton momentum of 1.82 ± 0.09 BeV/c and the target proton at rest. The momentum spread of the beam proton was obtained by transforming to the laboratory system the known proton momentum distribution in the beam deuteron rest system. The calculated distribution is approximated fairly closely by a Gaussian with $\sigma=0.09$ BeV/c.

The effect of ignoring the target motion in constraining reactions (1b) and (2) is to broaden the χ^2 distribution, relative to a χ^2 distribution for a genuine one-degree-of-freedom event. In a one-constraint fit the χ^2 value is approximately $[(M_M-M_N)/\Delta M_M)]^2$, where M_M is the calculated missing mass, M_N is the true mass of the outgoing neutral particle, and ΔM_N is the experimental error in missing mass.

Neglect of the target momentum $\mathbf{P}_T$ shifts the missing mass downward by an amount $(T_T T_n - \mathbf{P}_T\cdot\mathbf{P}_n)/M_M$, where T_T is the kinetic energy of the target particle and $\mathbf{P}_n$ and T_n are the momentum and kinetic energy of the outgoing neutral particle. There is a correlation between large χ^2 values and high momenta of the outgoing neutral particle. For this reason it was necessary to accept all nn and pp events with $\chi^2 \leqslant 10$.

The χ^2 criterion was used to identify the events only; we did not use the constrained values of the particle momenta because of the uncertainty in the target momentum. In calculating the (π^+p) and (π^-n) invariant masses we used the measured values of the particle momenta, and the neutron momentum was inferred from momentum conservation in reaction (1b) with the target neutron assumed to be at rest. The neutron momentum is then uncertain by $\mathbf{P}_T$, the target momentum, in addition to the usual measurement errors. In consequence, the calculated (π^-n) invariant mass, ω_{π^-n}, is reduced from its true value by

$$\Delta Q = [(E_\pi/E_n)(\mathbf{P}_n\cdot\mathbf{P}_T)-(\mathbf{P}_\pi\cdot\mathbf{P}_T)]/\omega_{\pi^-n}.$$

A Monte Carlo calculation shows that ΔQ has a distribution with mean of -0.2 MeV, and root-mean-square deviation 6 MeV; its effect on the mass and width of the (π^-n) distribution can therefore be ignored.

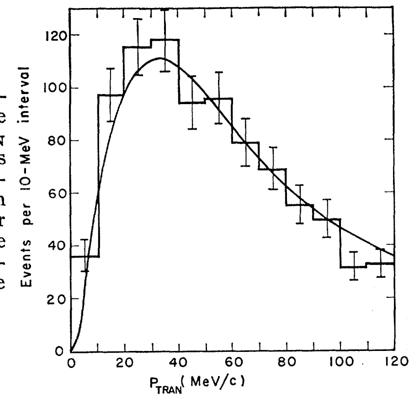

FIG. 1. Distribution in transverse momentum P_{TRAN} of spectator nucleons in the beam deuterons. The smooth curve is the Fourier transform of the Hulthén wave function, folded into the transverse plane.

Two additional criteria were applied to enforce a correspondence between the nn and pp events.

(a) There may be a scanning bias against pp events with a short proton track. So we eliminated pp events with $P_p<150$ MeV/c, and nn events with $P_n<150$ MeV/c.

(b) The uncertainty in ω_{23} due to measurement errors is greater for (π^-n) than for (π^+p). The average experimental error in ω_{23} is 30 MeV for (π^-n) and 20 MeV for (π^+p). We eliminated all events with an error exceeding 20 MeV. (No correlation was observed between ω_{23} and its error.) Then the experimental error is the same in both reactions, and is small comparted with the resonance width ($\Gamma_0=120$ MeV for N^{*++}). This condition is important because the value of the resonant mass inferred from the invariant-mass distribution is not independent of the width of the distribution.[16] A total of 1091 and 722 events satisfied the selection criteria for nn and pp interactions, respectively.

B. Subtraction of np Events in the Reaction $nd \rightarrow pp n\pi^-$

For the nn events in reaction (1b) the beam proton is a spectator; in the pn event the beam neutron is a spectator. A beam spectator is identified by having a momentum of less than 120 MeV/c in the rest system of the beam deuteron. The transverse momentum distribution of such nucleons is shown in Fig. 1; it follows closely the Hulthén form of the deuteron wave function, giving evidence for the validity of the impulse approximation. In a total of 1091 dn interactions, 133 had a beam spectator neutron and did not have a beam spectator proton. (In a strongly peripheral interaction, the interacting nucleon is sometimes indistinguishable from a spectator.) The (π^-n) effective-mass distribution for these 133 events is shown in Fig. 2. They are clearly $pn \rightarrow pp\pi^-$ reactions, as there is no evidence of N^{*-} production. According to the measured nucleon-nucleon

[16] J. D. Jackson, Nuovo Cimento 34, 1644 (1964). See also Table IV and Sec. IV below.

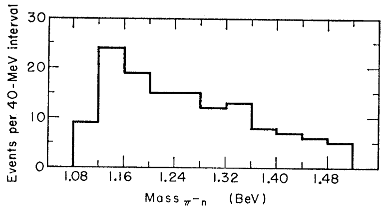

FIG. 2. The $(\pi^- n)$ invariant-mass distribution in the reaction $dn \to n_S{}^B pp\pi^-$, where $n_S{}^B$ is a spectator neutron in the beam deuteron.

cross sections in this energy region the ratio of nn to pn interactions is 5.2.[17] The expected number of pn events is then 176; the discrepancy is due to the experimental error in the neutron momentum which can shift it outside the limits for a high-energy spectator—$1.4<P<2.3$ BeV, 0 deg$<\theta<5$ deg—where P is the neutron momentum and θ is the angle it makes with the beam. The histogram in Fig. 2 was normalized to a total of 176 events and subtracted from the $(\pi^- n)$ invariant mass distribution (1091 events), to give the distribution in Fig. 3(a). Figure 3(b) shows the $(\pi^+ p)$ invariant-mass plot in the pp reactions.

III. POSSIBLE SOURCES OF ERROR

Since the N^{*-} mass is determined with a missing neutron whereas the N^{*++} is determined with two charged particles, systematic errors in the beam momentum or the magnetic field (or both) can simulate a mass difference. This danger is avoided by using the value of the beam momentum obtained by curvature measurement on beam tracks in the bubble chamber. If the magnetic field value is incorrect (say, by 1%), the pion and proton momentum are overestimated by 1%, but the neutron momentum is similarly affected, since it is calculated as $\mathbf{P}_n = \mathbf{P}_d - \sum \mathbf{P}_{\mathrm{charged}}$. So, there is no spurious mass difference induced by an incorrect value for the magnetic field, provided the beam momentum is estimated by use of the same value for the magnetic field.

A systematic sagitta in the chamber would change the beam momentum and shift the $(\pi^- n)$ invariant-mass distribution. The maximum systematic curvature in the chamber has been estimated at 0.1×10^{-4} cm^{-1}, equivalent to 1% of the beam momentum.[18] A 1% change in beam momentum causes an average shift of 1 MeV in the effective mass. In fact, there is strong evidence that the systematic curvature in the chamber is considerably less than the maximum value quoted.[18]

In reaction (1) target neutrons with momenta greater than 90 MeV/c are excluded. Hence the range of c.m. energies in reaction (1) is restricted compared with reaction (2). However, the requirement of a fit of reaction (2) has the effect of excluding high Fermi momenta. As a check on the equality of the range of interaction energies for the two reactions, the pion and nucleon momentum distributions are compared in Figs. 4(a), 4(b). The coincidence of the momentum spectra leads us to believe that there is no bias here.

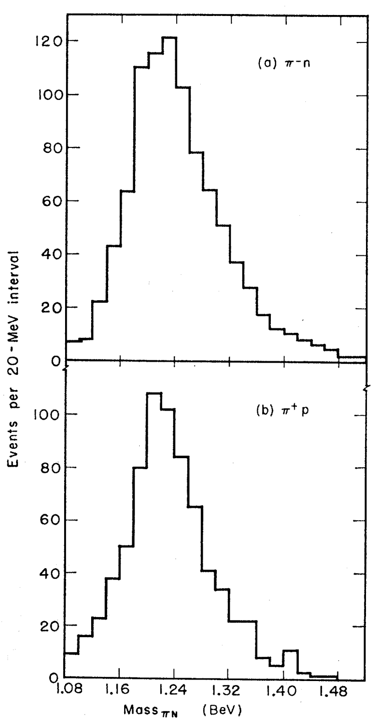

FIG. 3. (a) Distribution of the $(\pi^- n)$ invariant mass in the reaction $nn \to pn\pi^-$. (b) Distribution of the $(\pi^+ p)$ invariant mass in the reaction $pp \to np\pi^+$.

IV. DETERMINATION OF THE RESONANCE PARAMETERS

The differential cross section for reaction (1) is

$$d\sigma \propto |A|^2 \delta^4(P_f - P_i)(d^3p_1 d^3p_2 d^3p_3/E_1E_2E_3),$$

where A is the reaction amplitude. If A is known, one can calculate the $(\pi^- n)$ invariant-mass distribution $d\sigma(\omega,\omega_0,\Gamma_0)/d\omega$. The most probable values of ω_0 and Γ_0 are those which minimize χ^2 when the experimental

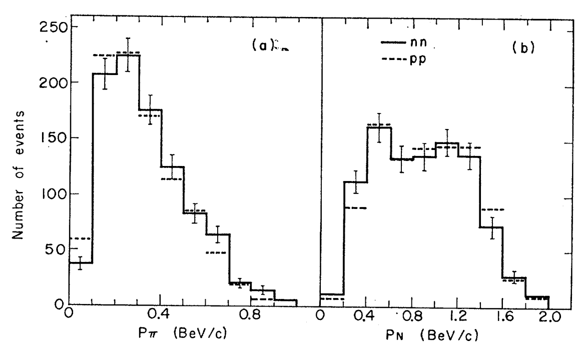

FIG. 4. (a) Normalized momentum distributions for π^- and π^+ in the reactions $nn \to np\pi^-$ and $pp \to np\pi^+$, respectively. (b) Normalized momentum distributions for neutrons and protons in the reactions $nn \to np\pi^-$ and $pp \to np\pi^+$, respectively.

---

[17] A. P. Batson, B. B. Culwick, H. B. Klepp, and L. Riddiford, Proc. Roy. Soc. (London), **A251**, 233 (1959).

[18] R. I. Louttit, in *Proceedings of the 1960 Conference on Instrumentation for High Energy Physics* (Lawrence Radiation Laboratory, Berkeley, California), p. 117.

distribution in ω is fitted with $d\sigma/d\omega$. Because the production mechanism is not completely understood, no absolute determination of ω_0 and Γ_0 is attempted in this experiment.

Since the two resonances are produced in charge-symmetric reactions, we assume that the mass difference can be evaluated by use of an approximate expression for the amplitude. The validity of the approximation is tested by comparing the calculated N^{*++} parameters with the values measured directly in π^+p elastic scattering.

Analyses of reactions (1) and (2) in this energy region[2,3] strongly indicate that: (a) the reactions go predominantly by one-pion exchange (OPE), and (b) the virtual π-nucleon scattering is dominated by the N^* resonant amplitude. We use these results to obtain an approximate expression for $d\sigma/d\omega$.

There are four OPE diagrams for reaction (1) (Fig. 5). The amplitude for the reaction is

$$A=A_a-A_b-A_c+A_d,$$

where the subscripts refer to the corresponding diagrams in Fig. 5. The interference terms $A_aA_d^*$ and $A_bA_c^*$ vanish because of the pseudoscalar nature of the pion, and it has been shown that the terms $A_aA_c^*$ and $A_bA_d^*$ are negligible.[19,20] Then

$$|A|^2=|A_a|^2+|A_b|^2-2\,\mathrm{Re}A_aA_b^* +|A_c|^2+|A_d|^2-2\,\mathrm{Re}A_cA_d^*.$$

It is convenient to split $d\sigma$ into the sum of six terms, corresponding to these six terms:

$$d\sigma=d\sigma_a+d\sigma_b+d\sigma_{ab}+d\sigma_c+d\sigma_d+d\sigma_{cd}.$$

In the pole approximation (exchanged pion on the mass shell) the partial cross section $d\sigma_a/d\omega$ is[21]

$$\frac{d\sigma_a}{d\omega}\propto\int_{\Delta_{\min}^2}^{\Delta_{\max}^2} k\omega^2\sigma(\omega)\frac{\Delta^2}{(\Delta^2+m_\pi^2)^2}d\Delta^2=\sigma(\omega)f(\omega), \quad (5)$$

where ω is the (π^-n) effective mass, k is the π^- momentum in the (π^-n) rest frame, Δ^2 is the square of the four-momentum of the exchanged pion, and $\sigma(\omega)$ is the cross section at the four-particle vertex. It is clear that $d\sigma_a/d\omega=d\sigma_b/d\omega$ and $d\sigma_c/d\omega=d\sigma_d/d\omega$. We evaluated $d\sigma_{ab}/d\omega$, using the expression for $d\sigma_{ab}$ derived by Selleri in the pole approximation[20] and found that $d\sigma_{ab}/d\omega\approx(0.6)\sigma(\omega)f(\omega)$. Since $d\sigma_{ab}/d\omega$ is almost identical in form with $d\sigma_a/d\omega$, we made the approximation

$$d\sigma/d\omega\propto d\sigma_a/d\omega+d\sigma_c/d\omega.$$

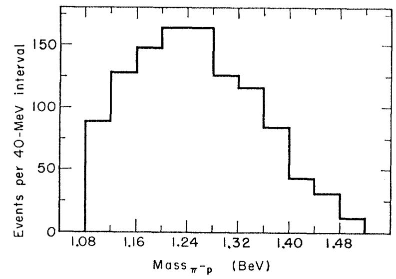

FIG. 6. The (π^-p) invariant-mass distribution in the reaction $nn\to pn\pi^-$.

Simple isotopic-spin considerations show that, in the case of N^* dominance, charged-pion exchange predominates over neutral-pion exchange in the proportions 9:1. Therefore 90% of the events in Fig. 3(a) correspond to N^{*-} production ($d\sigma_a$) and 10% to N^{*0} production ($d\sigma_c$). The shape of the (π^-n) effective-mass distribution for the $nn\to N^{*0}n$ events was approximated by the (π^-p) effective mass distribution in reaction (1) (Fig. 6). This distribution was normalized to 10% of the area in Fig. 3(a) and subtracted from it. The resulting distribution, shown in Fig. 7, corresponds to pure N^{*-} production and is described by $d\sigma_a/d\omega$. A similar procedure was used to eliminate the reflection of N^{*+} in the (π^+p) invariant-mass plot, giving the distribution in Fig. 7. The distributions in Fig. 7 contain a total of 695 nn and 558 pp events in the interval 1140 to 1320 MeV. These numbers do not reflect the relative cross sections, because not all photographs used for the nn interactions were scanned for pp interactions.

The distributions in Fig. 7 were fitted with Eq. (5),

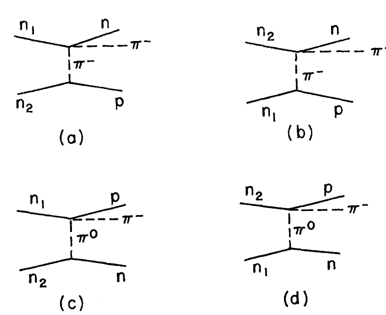

FIG. 5. Feynman diagrams for single-pion exchange in the reaction $nn\to pn\pi^-$.

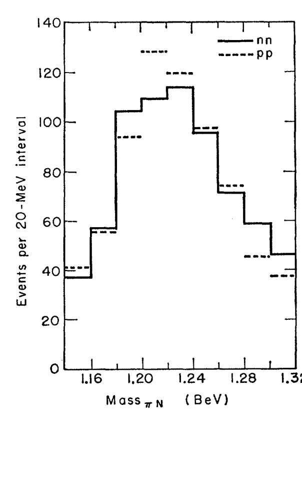

FIG. 7. Invariant-mass distributions of (π^-n) and (π^+p) in the reactions $nn\to np\pi^-$ and $pp\to np\pi^+$. The (π^+p) distribution (558 events) has been normalized to the area of the (π^-n) distribution (695 events).

[19] G. Da Prato, Nuovo Cimento **22**, 123 (1961).
[20] E. Ferrari and F. Selleri, Nuovo Cimento Suppl. **24**, 453 (1962).
[21] G. F. Chew and F. E. Low, Phys. Rev. **113**, 1640 (1959).

TABLE II. Masses, widths, and mass differences for N^* (all in MeV).

	With P-wave Breit-Wigner amplitude OPE[a]	With P-wave Breit-Wigner amplitude Phase space	With S-wave Breit-Wigner amplitude Phase space
Mass ω_0 N^{*-}	1241.3±5.1	1240.7±6.1	1219.7±3.4
N^{*++}	1233.4±4.4	1232.0±4.9	1217.4±3.2
Reduced width Γ_0 N^{*-}	149 ±18	166 ±21	133 ±13
N^{*++}	124 ±14	137 ±17	115 ±11
Mass difference $\delta\omega_0$	7.9±6.8	8.7±7.8	2.3±4.7
Width difference $\delta\Gamma_0$	25 ±23	29 ±27	18 ±17

[a] One-pion exchange.

modified by the off-mass-shell correction term[16]

$$\left[\frac{(\omega+m_2)^2+\Delta^2}{(\omega+m_2)^2-m_\pi^2}\right]^2\left[\frac{(\omega-m_2)^2+\Delta^2}{(\omega-m_2)^2-m_\pi^2}\right].$$

The upper limit for Δ^2 was set at 0.8 $(\mathrm{BeV}/c)^2$, according to the observed Δ^2 distribution in the nn reactions. In fact, the result is insensitive to a 50% variation in $\Delta_{\max}^2$. We use a single resonant p-wave amplitude for the π-nucleon cross section σ:

$$\sigma(\omega)\propto\omega_0^2\Gamma^2(\omega)/[(\omega_0-\omega)^2+\omega_0^2\Gamma^2(\omega)],$$

with

$$\Gamma=\Gamma_0(q/q_0)^3\rho(\omega)/\rho(\omega_0),$$

where $\rho(\omega)=(am_\pi^2+q^2)^{-1}$ and $a=1.3$ for m_π and q in MeV units[16]; q is the momentum of the decay products in the N^* rest frame. The values of ω_0 and Γ_0 which minimize χ^2 are shown in Table II. (It is reassuring that the N^{*++} parameters are in good agreement with the values measured in elastic π^+p scattering,[22,23] which are $\omega_0^{++}=1236\pm0.5$ MeV, $\Gamma_0^{++}=120\pm1.6$ MeV.)

In the absence of detailed knowledge of the reaction amplitude it is conventional to assume that the resonance and accompanying particles are produced according to phase space. This procedure is usually adequate for a narrow resonance ($\Gamma_0<50$ MeV). In Table II we give the resonance parameters obtained by fitting the distributions with the product of the three-body phase space and $\phi(\omega)$,[16] where $\phi(\omega)=C(\omega/q)\times\{\omega_0\Gamma(\omega)/[(\omega_0^2-\omega^2)^2+\omega_0^2\Gamma^2(\omega)]\}$; C is a normalization constant.

TABLE III. Error matrix for masses and widths in the OPE fit [all in $(\mathrm{MeV})^2$].

	ω_0^-	Γ_0^-	ω_0^{++}	Γ_0^{++}
ω_0^-	26.2	69.6	0.0	0.0
Γ_0^-	69.6	326.	0.0	0.0
ω_0^{++}	0.0	0.0	19.7	43.9
Γ_0^{++}	0.0	0.0	43.9	201.

[22] N. Klepikov, V. Meshcheryakov, and S. Sokolov, Joint Institute for Nuclear Research (Dubna) Report JINR-D-584, 1960 (unpublished).
[23] M. G. Olsson, Phys. Rev. Letters **14**, 118 (1965).

TABLE IV. Error matrix for mass and width differences in the OPE fit [all in $(\mathrm{MeV})^2$].

	$\delta\omega_0$	$\delta\Gamma_0$
$\delta\omega_0$	45.9	113.
$\delta\Gamma_0$	113.	527.

When, as for N^*, the width Γ is energy-dependent, the peak position in the invariant-mass plot, ω_{peak}, falls below ω_0, the shift $\omega_0-\omega_{\mathrm{peak}}$ being proportional to Γ_0^2. In order to locate the actual position of the peaks in the invariant-mass plots, we fitted them with an S-wave Breit-Wigner amplitude multiplied into phase space. This gives $\delta\omega_{\mathrm{peak}}=2.3\pm4.7$ MeV and $\delta\Gamma=18\pm17$ MeV. Since the width of the ω^- distribution exceeds that of ω^{++}, one expects that $\delta\omega_0$ will be greater than $\delta\omega_{\mathrm{peak}}$ when a P-wave Breit-Wigner form is used, and this is indeed the case.

The values obtained by the OPE fit, $\delta\omega_0=7.9\pm6.8$ MeV and $\delta\Gamma_0=25\pm23$ MeV, are taken as the best estimates of the resonance parameters. The error matrix for the masses and widths in the OPE fit is given in Table III, and for the mass and width difference in Table IV. There is a strong correlation between the estimated mass and width difference—the correlation coefficient is 0.73.

V. DISCUSSION

Within the $\frac{3}{2}^+$ decouplet, the following additional mass differences have been reported:

$$N^{*++}-N^{*0}=-0.45\pm0.85\text{ MeV}\quad\text{(Ref. 23)},$$
$$Y^{*-}-Y^{*+}=17\pm7\text{ MeV}\quad\text{(Ref. 24)},$$
$$Y^{*-}-Y^{*+}=4.3\pm2.2\text{ MeV}\quad\text{(Ref. 25)},$$
$$\Xi^{*-}-\Xi^{*0}=5.7\pm3.0\text{ MeV}\quad\text{(Ref. 26)},$$
$$\Xi^{*-}-\Xi^{*0}=7.0\pm4.7\text{ MeV}\quad\text{(Ref. 27)}.$$

These values, together with the value reported here, are compatible with relations (3) and (4), with pure octet dominance, and with the modified tadpole theory. In particular, the $SU(6)$ scheme predicts $\delta\omega_0=N^{*-}-N^{*++}=3.9$ MeV; pure octet dominance predicts $\delta\omega_0=9.0$ MeV; modified tadpole theory predicts $\delta\omega_0=4.9$ MeV. It is clear that our errors prevent us from distinguishing among theories with predictions in this range. The value predicted for $\delta\omega_0$ by using the measurements of Refs. 23 through 27 to evaluate the coefficients in Eq. (3) is $\delta\omega_0=5.0\pm1.5$.

[24] W. A. Cooper, H. Filthuth, A. Fridman, E. Malamud, E. S. Gelsema, J. C. Kluyver, and A. G. Tenner, Phys. Letters **8**, 365 (1964).
[25] Darrell O. Huwe, Ph.D. thesis, Lawrence Radiation Laboratory Report UCRL-11291, 1964 (unpublished).
[26] G. M. Pjerrou, P. E. Schlein, W. E. Slater, L. T. Smith, D. H. Stork, and H. K. Ticho, Phys. Rev. Letters **14**, 275 (1965).
[27] G. W. London, Dissertation Abstr. Vol. 3060 (1964).

ACKNOWLEDGMENTS

We wish to thank the many members of the staff of the Brookhaven National Laboratory whose help made the experiment possible. In particular, we express our appreciation to Dr. Hildred Blewett, Dr. Hugh Brown, Dr. Ralph Shutt, and the AGS operating crew. We are indebted to Dr. Robert Birge, Dr. Jonas Shultz, Dr. Robert Socolow, and Dr. Frank Solmitz for helpful discussions, and to Dr. Robert Ely and Dr. George Kalmus for their work during the bubble-chamber run. Finally, we thank the scanning and measuring staff of the Powell-Birge group and the Data Processing group under Howard White.

PHYSICAL REVIEW VOLUME 141, NUMBER 4 JANUARY 1966

Measurement of Proton Electromagnetic Form Factors at High Momentum Transfers*

K. W. Chen,† J. R. Dunning, Jr., A. A. Cone,‡ N. F. Ramsey, J. K. Walker, and Richard Wilson

Department of Physics, Harvard University, Cambridge, Massachusetts

(Received 9 June 1965; revised manuscript received 8 September 1965)

Elastic electron-proton scattering cross sections have been measured using the internal beam of the 6-BeV Cambridge Electron Accelerator at laboratory scattering angles between 31° and 90° for values of the four-momentum transfer squared ranging from $q^2=0.389$ to 6.81 $(\text{BeV}/c)^2$ ($q^2=10$ to 175F^{-2}). Incident electron energies ranged from 1.0 to 6.0 BeV. Scattered electrons from an internal liquid-hydrogen target were momentum-analyzed using a single quadrupole spectrometer capable of momentum analysis up to 3.0 BeV/c. Čerenkov and shower counters were used to help reject pion and low-energy background. The cross sections presented are absolute cross sections with experimental errors ranging from 6.8% to 20%. Separation of proton electromagnetic form factors have been made for all but the two highest momentum transfer points, using the Rosenbluth formula. Both form factors, G_{Ep} and G_{Mp}, were observed to continue to decrease as the momentum transfer increases. An upper limit to the possible asymptotic values of the proton electromagnetic form factors has been established.

I. HISTORY AND INTRODUCTION

With the advent of high-energy electron accelerators, it became feasible to utilize the scattering of electrons by hydrogen to yield precise and more complete information concerning the electromagnetic structure of nucleons. The pioneer work performed by Hofstadter and co-workers[1] first showed unambiguously that the proton is associated with a mean-square radius of the charge and magnetic distributions of about 1.0×10^{-13} cm. The differential cross sections, $d\sigma/d\Omega$, for the scattering of high-energy electrons by protons have been measured, and the data are analyzed by means of the well known Rosenbluth formula[2]

$$\frac{d\sigma}{d\Omega}=\sigma_{\text{Mott}}\frac{E'}{E}\left\{F_1{}^2(q^2)+\frac{q^2}{4M^2}\kappa_p{}^2F_2{}^2(q^2)+2\frac{q^2}{4M^2}[F_1(q^2)+\kappa_pF_2(q^2)]^2\tan^2(\tfrac{1}{2}\theta)\right\},\quad(1)$$

where σ_{Mott} is the cross section for scattering of electrons by a Coulomb field, q^2 is the square of the invariant four-momentum transfer, and $F_1(q^2)$ and $F_2(q^2)$ are the Dirac and Pauli form factors of the proton. These form factors are related to the mean-square radii of the charge, $\langle r^2\rangle_1$, and anomalous magnetic-moment distributions of the proton, $\langle r^2\rangle_2$, respectively, by

$$\langle r^2\rangle_{1,2}=\frac{1}{F_{1,2}(0)}\left(6\frac{\partial F_{1,2}(q^2)}{\partial q^2}\right)\bigg|_{q^2=0},\quad(2)$$

where $F_1(0)$ and $F_2(0)$ are the values of the form factors at zero momentum transfer. A major effort to measure the form factors has been under way for the last decade in many laboratories, at Stanford, Cornell, and Paris.[3–12]

* Work supported by the U. S. Atomic Energy Commission.

† Present address: Palmer Physical Laboratory, Princeton University, and Princeton-Pennsylvania Accelerator, Princeton, New Jersey.

‡ Present address: Southeastern Massachusetts Technological Institute.

[1] For a review of earlier work, see R. Hofstadter, *Nuclear and Nucleon Structure* (Benjamin Inc., New York, 1963).

[2] M. N. Rosenbluth, Phys. Rev. **79**, 615 (1950).

[3] F. Bumiller, M. Croissiaux, E. Dally, and R. Hofstadter, Phys. Rev. **124**, 1623 (1961).

[4] P. Lehmann, R. Taylor, and R. Wilson, Phys. Rev. **126**, 1163 (1962).

[5] D. Yount and J. Pine, Phys. Rev. **128**, 1842 (1962).

[6] B. Dudelzak, G. Sauvage, and P. Lehmann, Nuovo Cimento, **28**, 18 (1962).

[7] D. J. Drickey and L. N. Hand, Phys. Rev. Letters **9**, 521 (1962).

[8] K. Berkelman, M. Feldman, R. M. Littauer, G. Rouse, and R. R. Wilson, Phys. Rev. **130**, 2061 (1963).

[9] J. R. Dunning, Jr., K. W. Chen, N. F. Ramsey, J. R. Rees, W. Shlaer, J. K. Walker, and R. Wilson, Phys. Rev. Letters **10**, 500 (1963).

[10] K. Berkelman, M. Feldman, and G. Rouse, Phys. Letters **6**, 116 (1963).

[11] K. W. Chen, A. A. Cone, J. R. Dunning, Jr., S. G. F. Frank, N. F. Ramsey, J. K. Walker, and R. Wilson, Phys. Rev. Letters **11**, 561 (1963).

[12] B. Dudelzak, G. Sauvage, and P. Lehmann, Nuovo Cimento **28**, 14 (1963).